

**RESULTS ON ENVELOPE AND DISK DISPERSAL FROM A NEW MID-INFRARED SURVEY OF THE  $\rho$  OPH CLOUD CORE.** Mary Barsony, *Department of Physics & Astronomy, San Francisco State University and Space Science Institute*, Michael E. Ressler, *Jet Propulsion Laboratory*, Kenneth A. Marsh, *Jet Propulsion Laboratory*.

The mid-infrared wavelength range is especially relevant for studies of planet-forming disks since mid-IR emission peaks at distances of order  $\sim 1$  AU around most young stellar objects [YSOs], whereas the near-IR continuum originates from hot dust at  $\sim 0.1$  AU [1,2]. To study disk dissipation, as well as the evolution of the inner envelope regions in YSOs, we undertook a high angular resolution mid-IR imaging survey of the embedded YSO population in the nearby [d=125 pc]  $\rho$  Oph cloud core [3].

The target list of 172 objects was comprised of sources from the near-IR survey of Barsony et al. [4], that were bright,  $K \leq 13.0$  (since YSOs are generally bright NIR emitters), and highly reddened,  $H_K \geq 1.67$  (since large NIR excess is generally a disk indicator). These combined criteria guaranteed that the cloud core's embedded YSO population was completely sampled to an  $A_V \approx 21$ , even for young brown dwarfs. The source list was augmented by cloud members identified from studies at other wavelengths, but not meeting the above NIR selection criteria.

The mid-infrared imaging data of likely young  $\rho$  Oph cloud members were obtained over a span of 4 years (1996-1999) using 2 instruments (MIRLIN and LWS) on 3 telescopes (the Hale 5-meter and both Keck 10-meter telescopes). All observations at Palomar and on Keck II were made with MIRLIN [5], whereas observations at Keck I were made with LWS [6]. The MIRLIN data were acquired at N-band ( $\lambda_0 = 10.78\mu\text{m}$ ,  $\Delta\lambda = 5.7\mu\text{m}$ ). The LWS data were acquired through a narrower-band filter ( $\lambda_0 = 12.5\mu\text{m}$ ,  $\Delta\lambda = 1.0\mu\text{m}$ ) to avoid saturating the medium-well-depth detector of this instrument. MIRLIN has a plate-scale of  $0.138''/\text{pixel}$  and a  $17.7'' \times 17.7''$  field of view at the Keck II telescope; and a  $0.15''/\text{pixel}$  plate-scale and  $19.2'' \times 19.2''$  field of view at the Hale 5-meter. LWS had a plate-scale of  $0.08''/\text{pixel}$  and a field of view of  $10.2'' \times 10.2''$  at Keck I. For reference, the full-width at half-maximum of a diffraction-limited image at N-band is  $\sim 0.25''$  at the Keck telescopes and  $0.47''$  at the Hale 5-meter. Total on-source integration times were 25 seconds for MIRLIN and 72 seconds for LWS observations. Mean  $1-\sigma$  flux errors were  $0.018 \pm 0.024$  Jy with LWS on Keck I,  $0.008 \pm 0.005$  Jy at  $10.8\mu\text{m}$  with MIRLIN at Keck

II, and  $0.029 \pm 0.033$  Jy with MIRLIN at Palomar.

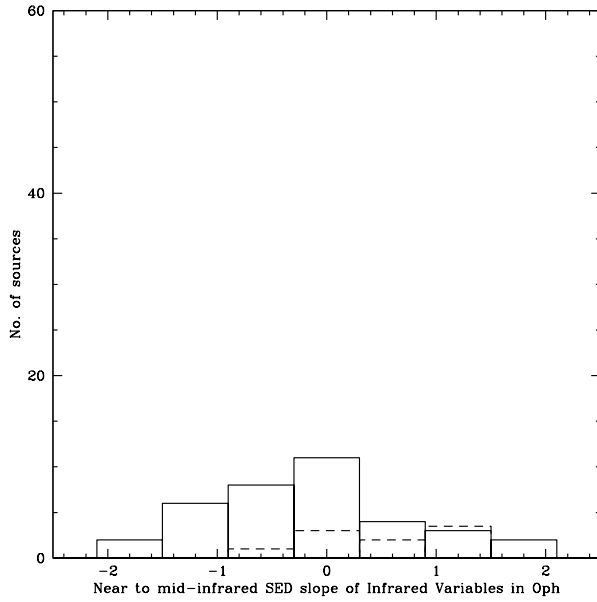
Of 172 survey objects, 85 were detected. There are 120 objects common to both this survey and the *ISOCAM* survey [7]. Of the sources in common to both surveys, 69 have both  $6.7\mu\text{m}$  and  $14.3\mu\text{m}$  fluxes determined from the *ISOCAM* survey. For these objects,  $10.8\mu\text{m}$  and  $12.5\mu\text{m}$  fluxes could be linearly interpolated from the *ISOCAM* data for direct comparison with the ground-based fluxes. The agreement is generally good between the two datasets, meaning that the ground-based fluxes agree with the *ISOCAM* fluxes to within  $3\sigma$  of the published uncertainties.

However, for a subset of the data, our flux measurements disagreed with previously published ground-based measurements or with the *ISOCAM* fluxes. These sources are candidate mid-infrared variables. A histogram of their SED (spectral energy distribution) slope,  $\alpha$ , is plotted in Figure 1. (See [3] for the definition of  $\alpha$ ). The SED slope distribution of known NIR variables (from BKLT) is indicated by the dashed histogram of Figure 1. Note that mid-IR variability occurs throughout all SED classes with detectable mid-IR emission. Near-IR variability also occurs throughout most SED classes.

Figure 2 shows the SED slope distribution of the objects detected in this survey (solid histogram) and of sources detected by the *ISOCAM* survey (dashed line). The large fraction of objects in the Flat Spectrum region of the graph ( $-0.3 \leq \alpha \leq +0.3$ ) in both datasets demonstrates that the Flat Spectrum, or envelope-clearing phase, in YSO evolution has a significant duration,  $\sim 4 \times 10^5$  yr.

A plot of the near-infrared (inner disk) excess vs. mid-infrared (outer disk) excess emission for single, well-resolved objects with known  $T_{eff}$  and  $A_V$  (not shown here) is consistent with disk clearing proceeding from the inside-out.

Funding from NSF grant AST-0206146 is gratefully acknowledged.



(2005), *ApJ*, 630, 381. [4] Barsony, M. et al. (1997) [BKL], *ApJS*, 112, 109. [5] Ressler et al. (1994), *Exp. Astr.*, 3, 277. [6] Jones, B. & Puetter, R. (1993), *Proc. SPIE*, 1946, 610. [7] Bontemps, S. et al. (2001), *A&A*, 372 173.

Fig. 1. Histogram of mid-IR (solid line) and near-IR (dashed line) variables as a function of YSO evolutionary stage,  $\alpha$ . Variability occurs throughout all YSO classes with optically thick disks.

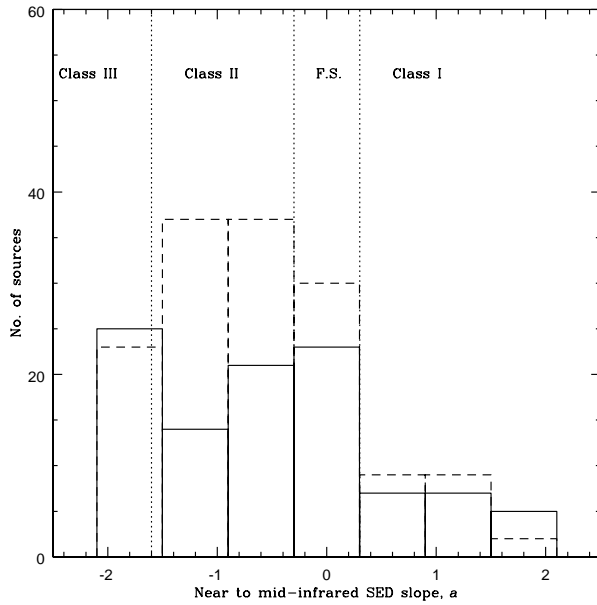


Fig. 2. Histogram of the observed distribution of  $\rho$  Oph sources among YSO stages: Solid line (this work), dashed line [7]. The large number of F.S. sources signals  $\sim 4 \times 10^5$  yr for envelope-clearing.

**References:** [1] Skrutskie, M. et al. (1990), *AJ*, 99, 1187. [2] Eisner, J.A. et al. (2003), *ApJ*, 588, 360. [3] Barsony, M., Ressler, M.E., & Marsh, K.A.